Surface & Coatings Technology 205 (2010) 2654–2660

Contents lists available at ScienceDirect

Surface & Coatings Technology

journal homepage: www.elsevier.com/locate/surfcoat

Microstructure analysis of plasma nitrided cast/forged CoCrMo alloys

Qingliang Wang *, Lei Zhang, Han Shen

School of Material Science and Engineering, China University of Mining and Technology, Xuzhou, Jiangsu 221116, China

ARTICLE INFO

Article history:
Received 29 July 2010
Accepted in revised form 11 October 2010
Available online 16 October 2010

Keywords:
Cobalt–chromium–molybdenum alloy
Plasma nitriding
Microstructure
Microhardness

ABSTRACT

Medical cast and forged CoCrMo alloys were coated by the plasma nitrided process to enhance the wear resistance. The microstructures, phases and microhardness of nitrided layers were studied by AFM, SEM, XRD and a micro-hardness meter. The experimental results showed that the plasma nitrided process has shown promise in producing thicker, harder, and more wear resistant layers than the conventional CoCrMo alloys. At low nitriding temperatures, the structures appeared to be consistent with the formation of S-phase, CrN phases in a parent structure of α-(CoCr) for the cast and forged alloy. At high nitriding temperatures, both cast and forged samples appeared to form CrN and Cr_2N as well as α-(CoCr) phases. Whether cast or forged CoCrMo alloy, the thickness of the nitrided layer increased with the nitriding temperatures. Moreover, the thickness of nitrided layers for forged alloys was higher than cast alloys under the same nitriding conditions. In the case of the cast and forged CoCrMo alloys, all plasma nitrided samples showed much higher hardness than the untreated samples.

1. Introduction

CoCrMo alloys are widely used for orthopedic applications such as hip and knee joint replacements [1,2]. The highly biocompatibility of the CoCrMo alloy is related closely to this material's excellent wear and corrosion resistance, imparted by a thin passive oxide film that forms spontaneously on the alloy surface. These films also form on the surfaces of other metal biomaterials, such as stainless steels and titanium alloys, and serve as a barrier to corrosion processes in alloy systems [3,4]. In spite of the excellent wear and corrosion resistance of the CoCrMo alloy, there is still a concern about wear debris and metal ion release (as wear or fretting and corrosion) from orthopedic implants into the body fluids, such as Co and Cr ions. These metal ions and wear debris, concentrated at the implant–tissue interface, may migrate through the tissue. Over time the level of metal ions may become clinically significant resulting in implant failure, osteolysis and allergic reactions [5,6].

Surface treatments are widely used for improvement of the biomaterial performances in order to enhance the mechanical properties or corrosion resistance and to reduce the possibility of implant failure and osteolysis [7,8]. As one of the important surface strengthening process, nitrogen ion implantation has been shown to improve wear resistance of orthopedic components such as the knee and hip replacements. Due to the formation of nitride precipitates, the implanted surface becomes harder. Hence, the wear resistance increases and the release of potentially harmful metal ions reduce [9,10]. However, due to the depth limitation, the orthopedics treated in such a way is quite costly and still the lifetime is limited. Since plasma assisted thermo chemical surface treatments improve wear, corrosion resistance and fatigue strength, the plasma nitriding or carburising CoCrMo alloy may be beneficial for the medical application [11–13]. But no much study about the plasma nitriding CoCrMo alloy is reported [14–17]. In the present study, the plasma nitriding method has been used to form the protective and wear resistance layer on the surface of the cast and forged CoCrMo alloy. The purpose of this study is to characterize the microstructures formed before and after plasma nitriding processing by X-ray diffraction, AFM and SEM. The microhardness measured by the micro-hardness meter is discussed.

2. Materials and methods

2.1. Material selection and preparation

Medical cast and forged cobalt–chromium–molybdenum (CoCrMo) alloys (ISO 5832-4 and ISO 5832-12) have been used in the experiments with the nominal compositions shown in Table 1. Disc specimens were cut from cylindrical bars with a diameter of 30 mm and a thickness of 5 mm. Before plasma nitriding, all the specimens were polished to a mean surface roughness of about 10–15 nm based on a 3D surface profiler. The samples were ultrasonically cleaned in an alcohol solution and deionized water for 15 min at room temperature, dried and stored under clean room conditions.

The specimens were placed into a holder which is the cathode of the plasma nitriding chamber. Prior to the process, the specimens were subjected to cleaning by argon sputtering for 30 min under a

* Corresponding author. Tel./fax: +86 516 83591916.
E-mail address: wql889@cumt.edu.cn (Q. Wang).

0257-8972/$ – see front matter © 2010 Elsevier B.V. All rights reserved.
doi:10.1016/j.surfcoat.2010.10.031

Table 1
Composition and mechanical properties of cast and forged CoCrMo alloys.

Material	Co	Cr	Mo	Ni	Fe	Mn	C	Tensile strength (MPa)	Yield strength (MPa)	Elongation (%)
Cast CoCrMo	bal.	28.7	6.18	0.38	0.73	0.61	0.21	690	465	8.5
Forged CoCrMo	bal.	28.2	5.98	0.41	0.70	0.64	0.23	840	590	17.5

Table 2
Treatment conditions of cast and forged CoCrMo samples.

Material	Sample no.	Plasma nitriding temperature (°C)	Current density (mA/cm^2)	Voltage (V)	Pressure of gas (Pa)	Nitriding time (h)	Roughness (Ra, nm)
Cast CoCrMo	Co0	Untreated	0	0	0	0	15
Cast CoCrMo	Co1	500	1.0	400	500	9	49
Cast CoCrMo	Co2	600	2.4	460	500	9	62
Cast CoCrMo	Co3	700	3.7	520	500	9	103
Cast CoCrMo	Co4	800	5.0	580	500	9	165
Forged CoCrMo	Co5	Untreated	0	0	0	0	11
Forged CoCrMo	Co6	500	1.0	400	500	9	51
Forged CoCrMo	Co7	600	2.4	460	500	9	59
Forged CoCrMo	Co8	700	3.7	520	500	9	72
Forged CoCrMo	Co9	800	5.0	580	500	9	77

voltage of 500 V and a pressure of 100 Pa. Then, the plasma nitriding was performed in gas of pure NH_3 (ammonia), with a constant pressure of 500 Pa and a process temperature of 500–800 °C and a process time of 9 h. Treatments were conducted using direct current and voltage between 400 and 600 V depending on the desired temperature. The detailed treatment conditions are listed in Table 2.

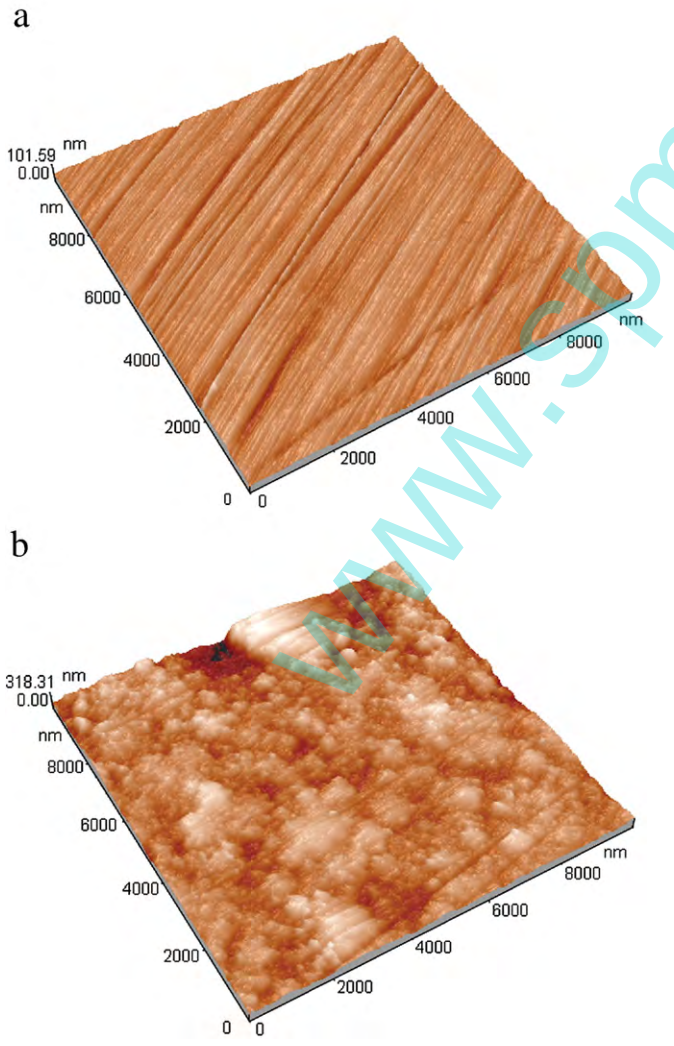

Fig. 1. AFM morphologies, (a) untreated cast CoCrMo and (b) nitrided cast CoCrMo at 700 °C.

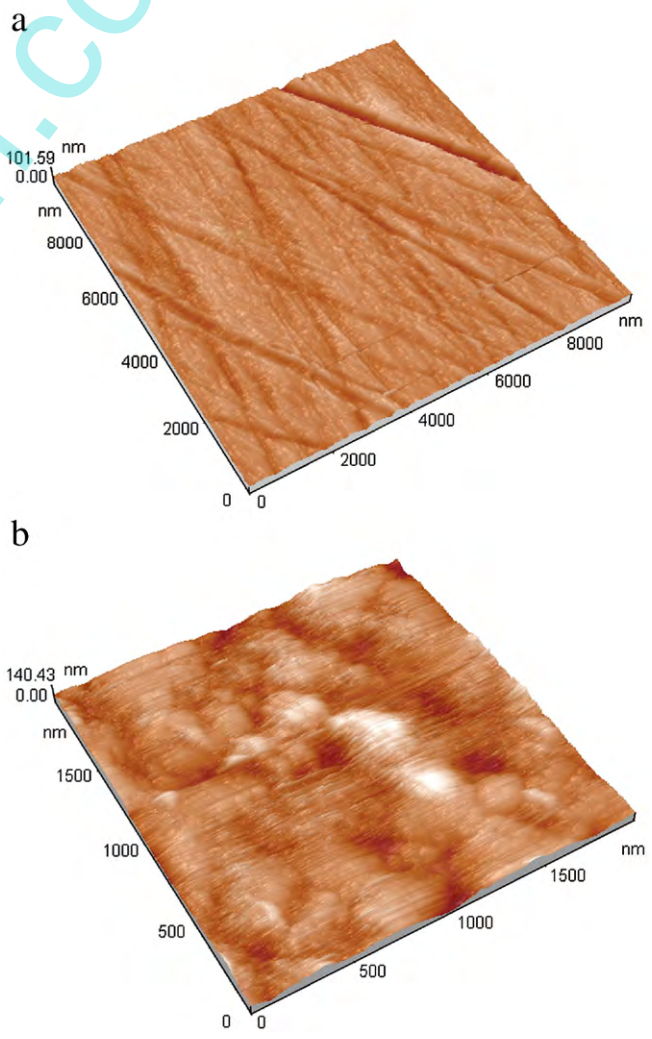

Fig. 2. AFM morphologies, (a) untreated forged CoCrMo and (b) nitrided forged CoCrMo at 700 °C.

2.2. Characterization techniques

Scanning electron microscopy (SEM, S3000, Hitachi Co., Japan) and atomic force microscopy (AFM, CSPM5500, China) were used to investigate the coating surface and cross-sectional morphologies for both untreated and nitrided specimens. X-ray diffraction (XRD, D/MAX-3B, Rigaku Co., Japan) was used for XRD analysis in a continuous-scanning mode (3°/min scanning velocity and 0.02° sampling spacing) with Cu-Kα radiation. The roughness of Ra was measured by an ultra-high-precision three-dimensional profiler (3D profiler, MiaoXAM2.5X-50X, USA). At least six readings were taken for each surface tested. The microhardness was measured by using a micro-hardness meter (HDX-1000, Taiming Test Co., China), with the applied load from 10 to 500 g.

3. Results and discussion

3.1. Morphology of AFM

AFM morphologies of untreated and nitrided cast and forged specimens are given in Figs. 1 and 2. It is observed that the surfaces are smooth and featureless, and there also appear some polished textures on surfaces of untreated samples. In contrast, shown in Figs. 1(b) and 2(b) are the images of cast and forged CoCrMo alloys nitrided at 700 °C. The surfaces become rougher due to the nitrogen ion bombardment. Using the 3D profiler, we also measured the roughness (Ra) of all cast and forged CoCrMo samples, which can be found in Table 2. For examples, the surface roughness of the untreated forged specimen was about 11 nm. But for the as-treated specimens, the surface roughness was measured from 51 nm to 77 nm. The cast one nitrided at 800 °C shows a highest roughness of about 165 nm in all nitride samples. Moreover, it has been also observed that the surface roughness increases with increasing the treatment temperatures due to ion bombardment.

3.2. Morphology of SEM

Shown in Fig. 3 are the SEM surface micrographs of cast CoCrMo samples treated under various conditions. All surfaces of treated samples are covered by the compact plasma nitrided layers composed of most nanoparticles. These nanoparticles less than 200 nm are uniformly distributed on the coating surfaces of the cast CoCrMo alloy. At a temperature above 700 °C, some larger size particles less than 1.5 μm can be found on plasma coatings shown in Fig. 3(c) and (d). Carefully observed, it can be seen that these large size particles are the micro-aggregates of nanoparticles. These results reveal that with the increase of plasma nitrided temperature, the nanoparticles of the nitrided coating are easy to aggregate and form some large size particles, which also results in the increase of surface roughness in Table 2. SEM images of plasma nitrided forged CoCrMo samples are given in Fig. 4. It is observed that the forged CoCrMo samples exhibit the quite similar morphologies as the cast samples. However, there appear some surface defects of micro-porous on the coating surfaces of the nitrided cast and forged samples.

3.3. Cross-sectional SEM

The cross-sectional SEM micrographs of untreated and plasma nitrided cast specimens are given in Fig. 5. At a low nitriding temperature in Fig. 5(b), a double layer structure formed the nitrided surface. The thickness of the first layer was measured about 6 μm and the second layer is about 3 μm. It is believed from XRD analysis that the second phase of CrN forms the first layer of the nitrided coating. The one below is the nitrogen diffused layer due to nitrogen atoms taking interstitial places among the parent structure and forming surface layers by expending the lattice. With an increase of the nitriding temperature, the possibility of the formation of CrN and Cr_2N

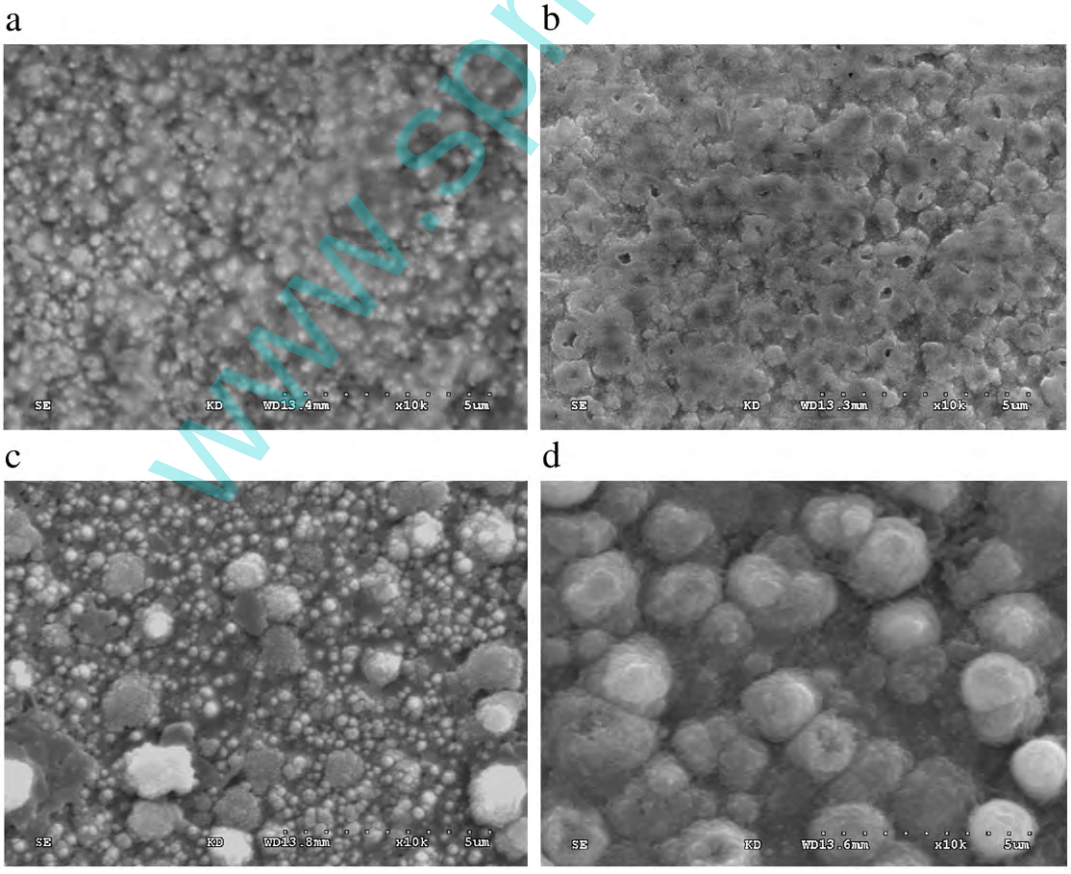

Fig. 3. SEM images of nitrided surfaces for cast CoCrMo samples (10,000×): (a) 500 °C, (b) 600 °C, (c) 700 °C and (d) 800 °C.

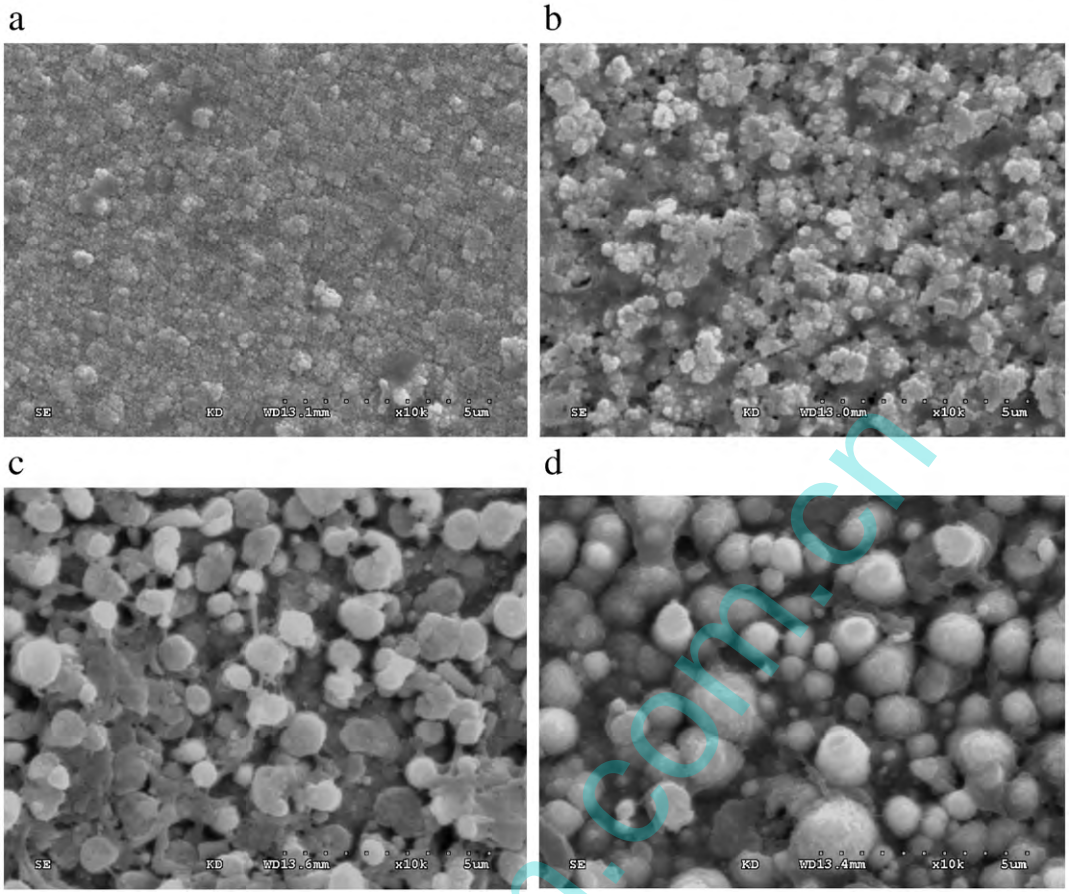

Fig. 4. SEM images of nitrided surfaces for forged CoCrMo samples (10,000×): (a) 500 °C, (b) 600 °C, (c) 700 °C and (d) 800 °C.

layer increases and therefore this layer dissolves. At a nitriding temperature of 700 °C shown in Fig. 5(c), only a widened nitride phase precipitate is seen to form uniformly throughout the parent microstructure, and the thickness of the nitrided layer increases to about 12 μm. In addition to these, the parent structure of the cast CoCrMo alloy appears to change at a high nitriding temperature. For untreated and nitrided samples at 500 °C, there is somewhat featureless for the substrate microstructure. However, there is clear evidence of lath microstructure in α-(CoCr) phase grains at 700 °C.

The cross-sectional micrographs for forged CoCrMo samples are shown in Fig. 6. Similar to the cast alloy, a double layer structure forms at a low nitriding temperature and a widened CrN phase precipitate forms at a high temperature. But the parent structure of the forged CoCrMo alloy appears to remain unchanged irrespective of the treatment temperature. Lath microstructures in α-(CoCr) phase grains are the typical features. In addition to these, the thickness of nitrided layers for the forged alloy is higher than the cast alloy under the same nitriding conditions. For examples, the thickness is about 12 μm at 500 °C (only about 9 μm for cast alloy), and then the thickness increases to about 17 μm at nitriding treatments up to 700 °C (only about 12 μm for cast alloy). However, it's observed that whether cast or forged CoCrMo alloy, the thickness of the nitrided layer increases with the nitriding temperatures.

3.4. XRD analysis

The XRD results for cast CoCrMo specimens are shown in Fig. 7. For the untreated sample, the structure appears to be a mixture of α-(CoCr) and ε-(CoCr) cobalt parent structure with solid solution chromium and molybdenum. There is a higher concentration of the ε-(CoCr) phase or ratio of ε/α. The presence of the ε-(CoCr) phase with a HCP (close-packed hexagonal, referred to as HCP) structure is consistent with the equilibrium Co/Cr phase diagram. The presence of α-(CoCr) existing in a FCC (face-centered cubic, referred to as FCC) structure above 450 °C is indicative of possibly a non-equilibrium transformation during cooling. Distinctive phases of the nitrided specimens which are CrN, Cr_2N and S-phase, depend on the treatment temperature. At a treatment temperature of 600 °C, it is observed that the ε-(CoCr) phase disappears and the CrN phase forms at peaks of about 37.2 and 62.8°. When the temperature increases to 700 °C, the S-phase occurs at the nearly same angles of the ε-(CoCr) phase. There are the clear diffraction peaks of the Cr_2N phase at about 44.2 and 55.1°. After the temperature up to 800 °C, it is clearly seen that the S-phase almost disappears and the main phases are α-(CoCr), CrN and Cr_2N for the nitrided cast alloy.

The XRD results for the untreated and nitrided forged CoCrMo alloy are shown in Fig. 8. Similar to the cast alloy, the untreated forged alloy consists of a two-phase mixture of α-(CoCr) and ε-(CoCr) cobalt phases although there is a higher concentration of the α-(CoCr) phase or ratio of α/ε. At low nitriding temperatures of 500 °C and 600 °C, there appears the transformation to a two-phase mixture of α-(CoCr) and S-phase, and there is also the formation of CrN (peak at 62.5). At higher temperatures of 700 °C and above, there is not only the presence of the parent α phase along with CrN, but there also appears to be the formation of the Cr_2N (40.2, 42.8 and 55.2) phase as well. In addition to these, S-phase disappearance at the specimens treated above 700 °C should be noted.

Lanning and Wei observed CrN and Cr_2N phases for the cast and forged CoCrMo alloy [14]. However, Celik et al. reported that the Co_2N phase was formed for forged alloy at 600 °C, in addition to CrN and Cr_2N phases [16]. As can be seen in Figs. 6 and 7, CrN and Cr_2N phases are found and the Co_2N phase cannot be occurring in the nitriding

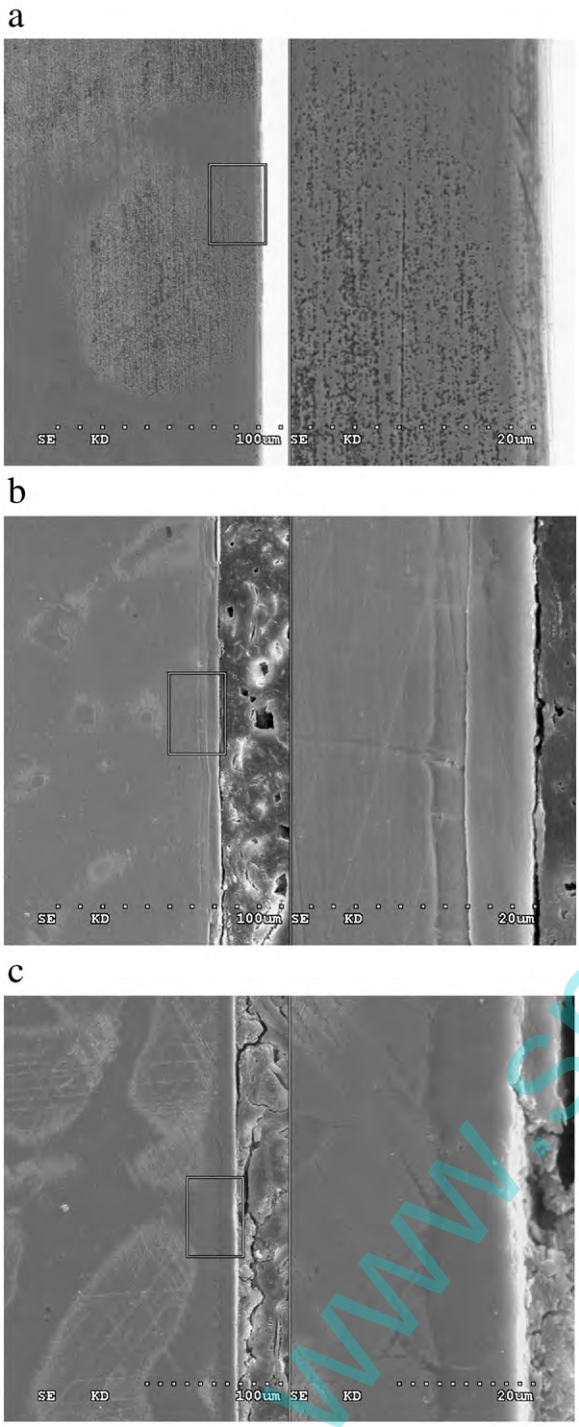

Fig. 5. Cross-sectional SEM images of cast CoCrMo samples: (a) untreated, (b) 500 °C and (c) 700 °C.

layers of the cast and forged CoCrMo alloys at different treatment temperatures. At the lower nitriding temperatures, the structures appear to be consistent with the formation of the S-phase, CrN phases in a parent structure of α-(CoCr). The S-phase is a metastable and interstitial supersaturated phase, which can form at low temperatures by introducing interstitials (such as N and C) into an FCC structured substrate with a certain amount of nitride/carbide formers. The S-phase surface engineering technology can pave the way towards long life, high performance joint bearing surfaces, especially for metal on metal configurations [18]. At the higher treatment temperatures, there is an apparent transformation to the phases of CrN and Cr_2N as

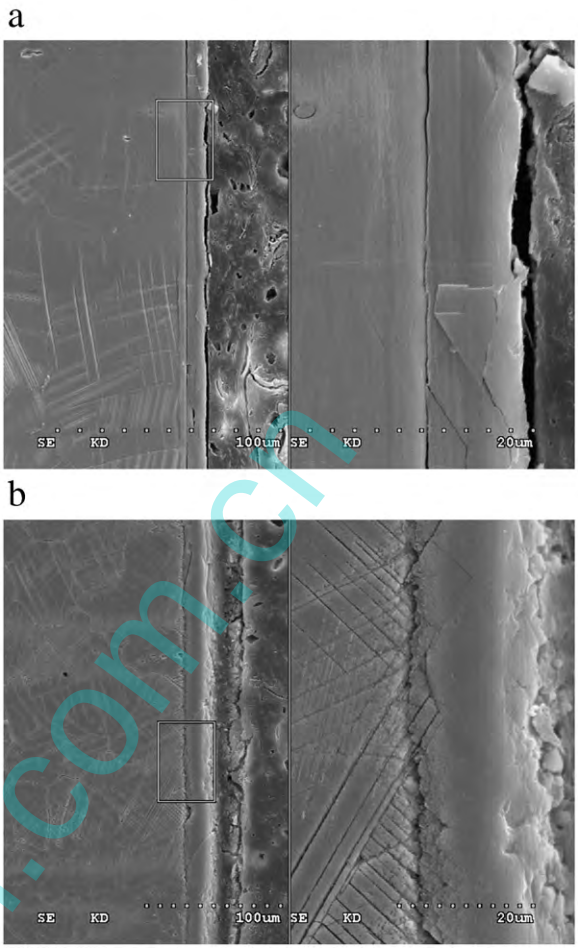

Fig. 6. Cross-sectional SEM images of forged CoCrMo samples: (a) 500 °C and (b) 700 °C.

well as the α-(CoCr) parent structure. Since the cast and forged CoCrMo samples have different fractions of α-(CoCr) and ε-(CoCr) parent phases, the degree and mechanism for nitrogen incorporation are slightly different at the intermediate temperatures. In addition to these, the increase of the Cr_2N phase content and the disappearance of the S-phase occur with an increase of the treatment temperatures. Since the S-phase is a cobalt rich phase, the formation of the S-phase requires either a higher concentration of cobalt or a higher temperature according to the Co/Cr phase diagram. It has been

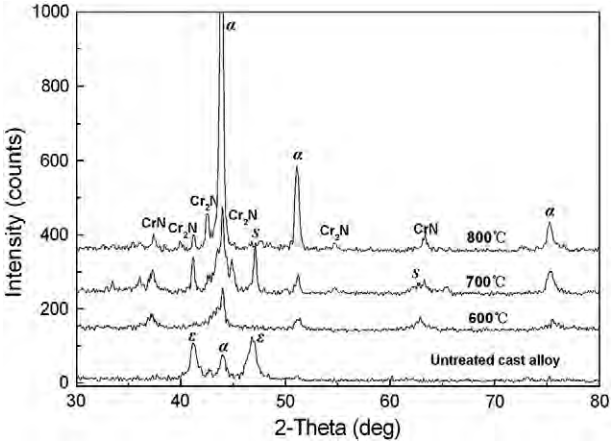

Fig. 7. XRD spectra for untreated and nitrided cast CoCrMo alloys.

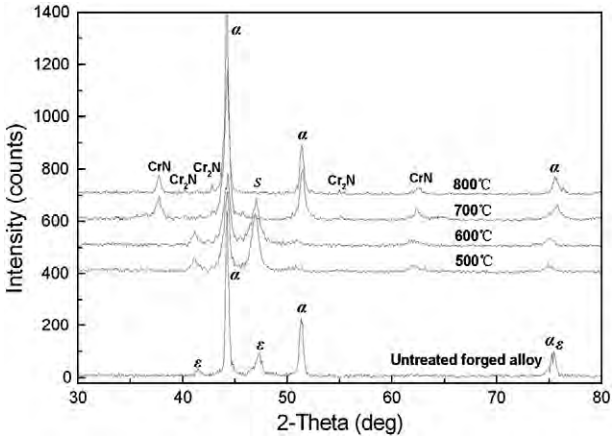

Fig. 8. XRD spectra for untreated and nitrided forged CoCrMo alloys.

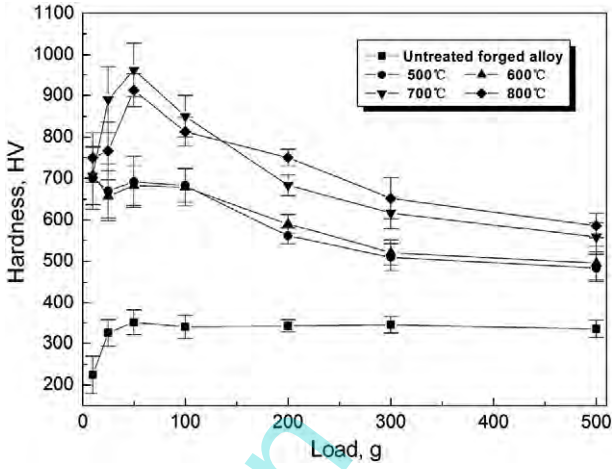

Fig. 10. Microhardness of untreated and nitrided forged CoCrMo alloys.

observed that the amounts of Cr_2N increase with an increase of the treatment temperature, which may induce the decomposition of chromium from the S-phase. Thus chromium atoms may bond with N atoms and form the Cr_2N phase. Clearly, the effects of the nitriding and elevated temperature have altered the distribution of phases at temperatures above 700 °C.

3.5. Microhardness

Figs. 9 and 10 present the apparent surface Vickers microhardness (HV) as a function of the applied load from 10 to 500 g. The hardness number is the average of 6 data points. It's observed that all the hardness of nitrided cast and forged samples is still much higher than the untreated samples at different loads. The plasma nitrided samples at high temperatures exhibit high hardness. But the sample treated at 700 °C shows the highest hardness for the nitrided cast alloy, and the highest value is at a nitriding temperature of 800 °C for the nitrided forged samples. This higher hardness for the nitrided CoCrMo alloy is believed to be due to the formation of CrN and Cr_2N mixed phases consisting of nano-crystalline structures. Although, some authors have assigned this behavior to the presence of nano-crystalline inside the coatings, this result is also due to the intrinsic hardness of the deposited compound [19]. It's worth noting that the plasma nitrided cast alloys show the highest hardness at 700 °C. At temperatures less than 700 °C, S-phase and CrN are the new generated phases. The higher hardness of the CrN phase ($HV_{0.05}=2740$) increases the hardness of the nitriding CoCrMo alloy. But, the hardness of the S-phase is similar or even harder than quenched Fe–C (950HV) or Fe–N (800HV) [18]. At a nitriding temperature of 700 °C, the content of the harder CrN phase almost reaches the maximum and the S-phase decreases and disappears, which further enhances the hardness of the nitriding cast CoCrMo alloy. After the nitriding temperature is up to 700 °C (such as 800 °C), the Cr_2N phase appears in the nitrided surface. Its hardness ($HV_{0.05}=2175$) is lower than the hardness of CrN [20], which leads to lower the hardness of the nitriding CoCrMo alloy.

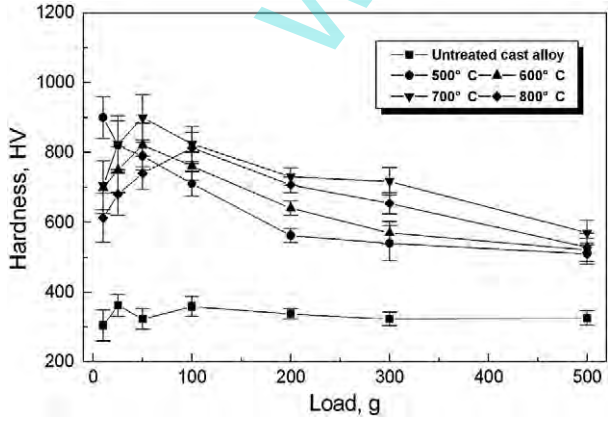

Fig. 9. Microhardness of untreated and nitrided cast CoCrMo alloys.

4. Conclusion

The plasma nitrided process has shown promise in producing thicker and harder layers than the conventional CoCrMo alloy. From the results presented in this paper, the improvement is attributed to deep nitrogen diffusion and hard nitride formation of CrN and Cr_2N phases (above 700 °C) in cast and forged CoCrMo alloys. At the lower nitriding temperatures, the structures appear to be consistent with the formation of S-phase, CrN phases in a parent structure of α-(CoCr) for the cast and forged alloy. At the higher treatment temperatures, both cast and forged samples appear to form CrN and Cr_2N as well as α-CoCr phases. Since the cast and forged CoCrMo samples have different fractions of α-(CoCr) and ε-(CoCr) parent phases, the degree and mechanism for nitrogen incorporation are different at the intermediate temperatures. In the case of cast and forged CoCrMo alloys, plasma nitrided samples exhibit much higher hardness than untreated samples. It was concluded that an increase of the hardness, as a result of plasma nitriding processing, can be related to both the formation of deep nitrided layers and the formation of specific nano-crystalline microstructures at the surfaces for both cast and forged alloys.

Acknowledgements

The authors thank the supports by the Tribology Science Fund from State Key Laboratory of Tribology (SKLT) at Tsinghua University (SKLTKF08A01) and the Natural Science Foundation of Jiangsu Province (BK2008005).

References

[1] R. Varano, J.D. Bobyn, J.B. Medley, S. Yue, J. Biomed. Mater. Res. B Appl. Biomater. 76 (2006) 281.
[2] S. Pramanik, A.K. Agarwal, K.N. Rai, Trends Biomater. Artif. Organs 19 (2005) 15.
[3] Y. Okazaki, E. Gotoh, Biomaterials 26 (2005) 11.
[4] A. Kocijan, I. Milošev, B. Pihlar, J. Mater. Sci. Mater. Med. 15 (2004) 643.
[5] A.P. Serro, M.P. Gispert, M.C.L. Martins, P. Brogueira, R. Colaço, B. Saramago, J. Biomed. Mater. Res. A 78 (2006) 581.
[6] I. Milošev, H.-H. Strehblow, Electrochim. Acta 48 (2003) 2767.
[7] J.R. Goldberg, J.L. Gilbert, Biomaterials 25 (2004) 851.
[8] U. Türkan, O. Öztürk, A.E. Eroğlu, Surf. Coat. Technol. 200 (2006) 5020.

[9] D. Ikeda, M. Ogawa, Y. Hara, Y. Nishimura, O. Odusanya, K. Azuma, S. Matsuda, M. Yatsuzuka, A. Murakami, Surf. Coat. Technol. 156 (2002) 301.
[10] Z. Werner, M. Barlak, M. Grądzka-Dahlke, R. Diduszko, W. Szymczyk, J. Dąbrowski, J. Piekoszewski, K. Borkowska, Vacuum 81 (2007) 1191.
[11] A. Alsaran, I. Kaymaz, A. Çelik, F. Yetim, M. Karakan, Surf. Coat. Technol. 186 (2004) 333.
[12] J. Chen, X.Y. Li, T. Bell, H. Dong, Wear 264 (2008) 157.
[13] X.Y. Li, N. Habibi, T. Bell, H. Dong, Surf. Eng. 23 (2007) 45.
[14] B.R. Lanning, R. Wei, Surf. Coat. Technol. 186 (2004) 314.
[15] R. Wei, T. Booker, C. Rincon, J. Arps, Surf. Coat. Technol. 186 (2004) 305.
[16] A. Celik, Ö. Bayrak, A. Alsaran, İ. Kaymaz, A.F. Yetim, Surf. Coat. Technol. 202 (2008) 2433.
[17] J. Lutz, S. Mändl, Nucl. Instrum. Methods Phys. Res. Sect. B 267 (2009) 1522.
[18] H. Dong, Int. Mater. Rev. 55 (2010) 65.
[19] S. Veprek, A. Niederhofer, K. Moto, T. Bolom, H.-D. Männling, P. Nesladek, G. Dollinger, A. Bergmaier, Surf. Coat. Technol. 133–134 (2000) 152.
[20] G. Bertrand, H. Mahdjoub, C. Meunier, Surf. Coat. Technol. 126 (2000) 199.